

Supplementary material

BMVC 2016 Submission # 158

1 PSF refinement

In this section, we provide a visual illustration of the PSF refinement process as discussed in section 3.5. Figs. A.1 (a) and (b) are, respectively, the ground truth PSF used for blurring the image and the estimated PSF. Fig. A.1 (c) shows the refined PSF. Note that filtering the PSFs estimated through weighted PCA brings them closer to ground truth. This step aids in finding better initial estimates for the virtual depth parameters and the latent image.

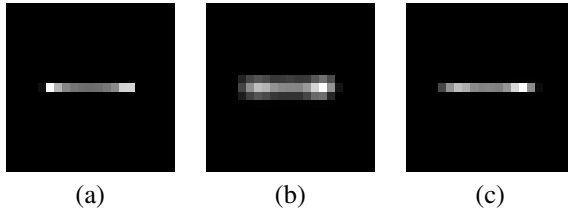


Fig A. 1: PSF refinement. (a) Ground truth, (b) PSF estimated using [21], and (c) refined PSF.

2 Shot detection

In this section, we describe a synthetic experiment demonstrating the importance of shot detection. We used the image in Fig. A.2 (a) and also an exponentially decaying periodic water surface with $\mathbf{V}_{dp1} = ([0.3162 \ 0.9487]^T, -0.0015)$ for the first 256 frames and $\mathbf{V}_{dp2} = ([1 \ 0]^T, -0.002)$ for the next 256 frames. We employ our shot detection module on the entire video and select the top two segments with least E_r (we knew a priori that only two stacks are possible). The blurred images generated by averaging the frames in each group and as returned by our shot detection framework are shown in Figs. A.2 (b) and (c). Fig. A.2 (d) shows the restored result by our proposed AM framework without shot detection. The restored results corresponding to the blurred images in Figs. 2 (b) and (c) are shown in Figs. A.2 (e) and (f), respectively, while Figs. 2 (g) and (h) shows the corresponding estimated virtual depth maps. It can be clearly seen that there are many artifacts in Fig. A.2 (d) (see highlighted patches in red, green, and blue colors) while the deblurred results (Fig. 2 (e,f)) obtained using our shot-detection scheme as a pre-processing step are closer to the ground truth.

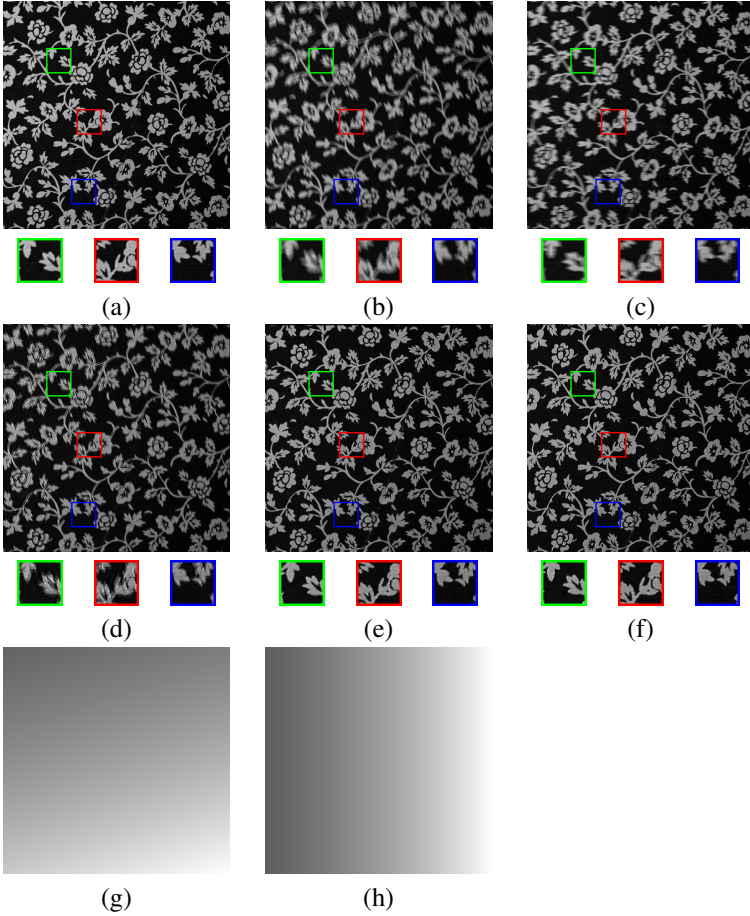


Fig A. 2: Significance of shot detection. (a) Ground truth. Blurred images generated by (b) segment 1, (c) segment 2. Restored observations: (d) without shot detection, (e) with shot detection for segment 1, and (f) with shot detection for segment 2. Virtual depth maps of (g) segment 1, and (h) segment 2.

3 Choice of parameters

In Eq. 9, all the weights related to the derivative terms are adopted from [1], whereas the values of $\lambda_{\theta_0}^{\omega}$ and λ_{ω} were found empirically as 0.1 and 1, respectively. Similarly, in Eq. 11, we adopt $\lambda_{\delta_*}^{\mathbf{d_p}}$ from [1], whereas the optimal values of both $\lambda_{\theta_0}^{\mathbf{d_p}}$ and $\lambda_{\mathbf{d_p}}$ were found empirically to be 1. During the estimation of latent image by using Eq. 13, the value of λ_{rs} is adopted from [16], while the value of λ_f is chosen as 0.001.